arXiv:1602.02335v2 [physics.ins-det] 7 May 2018

Photon flux and bunching noise from measurement of the shot noise variance

Richard Lieu[1], Michael Stefszky[2], and Johann, C. -H. Shi[3]

[1]*Department of Physics, University of Alabama, Huntsville, AL 35899*
[2]*Integrated Quantum Optics, University of Paderborn, Warburger Strasse 100, 33098 Paderborn, Germany.*
[3]*National Astronomical Observatories, Chinese Academy of Sciences, A20 Datun Road, Chaoyang District, Beijing 100012, China*

ABSTRACT

We report the experimental observation of photon bunching noise through shot noise measurements made on a pseudo-thermal state of light using balanced detection. A full theory describing the measurement is developed, and in agreement with theory it is found that the shot noise variance in the balanced signal reproduces the time series of the flux of the primary incoherent beam. Moreover, when the average power of the pseudo-thermal light is varied, the balanced detection is seen to track this change. A comparison of direct detection and balanced detection of the thermal field, shows that the balanced detection performs at least as well the direct detection and under some conditions appears to outperform the direct detection. There is not necessarily a contradiction with quantum field theory which predicts that at best the performance of the balanced detection should be equal to the direct detection, because the direct detection process is subject to nonlinearity that has not been excluded by measurements (even though any tests we performed suggest such effects are small). This is the first time that the bunching noise effect of high occupation number chaotic light via the shot noise of the field has successfully been measured, to the point of using it to infer the flux of the field. The findings may be relevant to radio receiver design, specifically from the viewpoint of sensitivity improvement.

1. Introduction

In Hanbury-Brown Twiss intensity interferometry Hanbury-Brown & Twiss (1957), when a stationary light beam of high occupation number is divided by a 50:50 beam splitter, the bunching noise (or classical wave phase noise) patterns in the intensity time series of

the two output beams are identical, because the beam splitter causes only a relative phase difference of π in the amplitudes of the two beams. This wave aspect of light has extensively been studied over the years, see *e.g.* Mandl & Wolf (1995). However, due to the indivisibility of photons, the other noise component, the shot noise Rice (2016), in each output beam is not expected to correlate between the two beams. Hence a subtraction of the time series of one output beam from another should yield a zero mean flux, but a flux variance that is another measure of the flux of the original (primary) beam at any given instance. Recently it has been shown, based on quantum field theory, that such a method of flux determination can in principle be as accurate as, though not surpassing, direct detection (here-and-after simply referred to as DD); in particular, it can reveal the bunching noise in the flux of the primary beam just as clearly as direct detection Zmuidzinas (2015); Lieu & Kibble (2015); Nair & Tsang (2015).

The purpose of the work presented here is to experimentally demonstrate, for the first time, the theoretically expected performance of flux measurement via the shot noise in the field. The shot noise is measured using a balanced detection (here-and-after simply referred to as BD) scheme, consisting of a 50:50 beamsplitter followed by the subtraction of the two photocurrents detected at each beamsplitter output. In this way we demonstrate a qualitative test for the predictions of quantum field theory and highlight an alternative method for radiometry. Whilst balanced detection requires greater experimental complexity than direct detection, it may come with other advantages such as the ability to negate large DC and low frequency noise components (such as from electronics) due to the fact that no DC information is required in the balanced scheme.

It might first be useful to seek a heuristic understanding of key predictions Zmuidzinas (2015); Lieu & Kibble (2015); Nair & Tsang (2015). Since there are classical bunching noise fluctuations in chaotic light, for any sufficiently short interval within which this noise is constant, the shot noise mean and variance (as could be measured with a single detector) should both equal the expected instantaneous photon count rate as determined by the bunching noise pattern there. In this way the shot noise will then exhibit a time dependent mean and variance as its amplitude adjusts in tandem with bunching. According to Zmuidzinas (2015); Lieu & Kibble (2015); Nair & Tsang (2015), this correlation between the shot noise variance and the classical noise intensity is not expected to be removed by the subtraction in the balanced detector, as illustrated in Figure 1. This is why a time series of the shot noise variance, as measured by the BD setup, is expected to trace the primary flux, including its bunching noise.

2. Quantum field theoretic prediction of noise behavior in chaotic light

We now discuss the specific quantum-field theory predictions.

2.1. Fully incoherent light

First is the theoretical expression of the ratio of the intensity covariance to the square of the mean intensity for stationary light. If the light is fully incoherent with a Gaussian autocorrelation function of width τ, eq. (9) of Lieu & Kibble (2015) indicates that for an intensity dataset S_k (J_k in Lieu & Kibble (2015)) directly measured by a radiometer the ratio is

$$\frac{\mathrm{cov}(S_k, S_l)}{\langle S_k\rangle^2} = e^{-t_{kl}^2/\tau^2}; \tag{1}$$

while for the BD squared difference current, eq. (32) of Lieu & Kibble (2015) yielded

$$\frac{\mathrm{cov}(D_k^2, D_l^2)}{\langle D_k^2\rangle^2} = e^{-t_{kl}^2/\tau^2} + 4\delta_{kl}. \tag{2}$$

In both equations $\mathrm{cov}(A, B) = \langle AB\rangle - \langle A\rangle\langle B\rangle$ with $\langle\cdots\rangle$ denoting ensemble mean, τ is the coherence time or inverse bandwidth of the incoherent light, and $t_{kl} = (k-l)T$ with T being one interval of sampling $T < \tau$ but long enough to collect $\gg 1$ photons per interval. Thus

$$\hat{S}_k = \frac{1}{T}\int_{(k-1)T}^{kT} dt\, \hat{S}(t) \tag{3}$$

with a similar expression for $\hat{D}_k^2$.

To interpret (1) and (2), one may revisit Figure 1. In the top schematic, the direct time series, the rapid fluctuations of the shot noise is seen to be dominated by the slower bunching noise variation, the characteristic width of the latter is τ and is given by one of the broad peaks shown (the insignificance of the shot noise is due to the assumption that the light has high photon occupation number, *i.e.* the number of photons per interval τ is $\gg 1$). Thus the autocorrelation function of S_k has as its chief feature a Gaussian of width τ. On the other hand, the bottom schematic of Figure 1 shows that the BD time series has shot noise and bunching noise of approximately the same strength; the former has a sharp autocorrelation function spanning one bin width T, while the latter has width τ which spans many intervals T but height equal to the former.

Moreover, (1) shows that for direct radiometry the variance obtained by setting both k and l to the same index j relates to the mean squared intensity as

$$\frac{\mathrm{var}\langle S_j\rangle}{\langle S_j\rangle^2} = 1; \tag{4}$$

while the same for (2) shows that for a BD measurement

$$\frac{\mathrm{var}\langle D_j^2\rangle}{\langle D_j^2\rangle^2} = 5. \tag{5}$$

In the extreme opposite limit of flux estimation, by averaging over a large interval $\mathcal{T} = NT$ comprising $N \gg 1$ intervals of T, (1) gives

$$\frac{\mathrm{var}(\overline{S_\mathcal{T}})}{\langle \hat{S}_j\rangle^2} \approx \frac{\sqrt{\pi}\tau}{\mathcal{T}} = \frac{\sqrt{\pi}\tau}{NT}; \tag{6}$$

while (2) gives

$$\frac{\mathrm{var}(\overline{D_\mathcal{T}^2})}{\langle \hat{D}_k^2\rangle^2} = \frac{1}{N}\left(\frac{\sqrt{\pi}\tau}{T} + 4\right), \tag{7}$$

where

$$\overline{S_\mathcal{T}} = \frac{1}{N}\sum_{k=1}^{N} S_k \tag{8}$$

and

$$\mathrm{var}(\overline{S_\mathcal{T}}) = \frac{1}{N^2}\sum_{k,l=1}^{N} \mathrm{cov}(S_k, S_l); \tag{9}$$

and similar expressions for $\overline{D_\mathcal{T}^2}$.

Now (6) is the radiometer equation for the ultimate sensitivity limit of the direct flux detection of fully incoherent light of high occupation number, a limit set by the bunching noise in the direct time series. The underlying physics is simply that bunching noise variances add on timescales greater than the coherence time τ, when the different segments of the time series have become independent (as seen in the top half Figure 1). Evidently, (7) indicates that on sufficiently long timescales $\mathcal{T}$ the sensitivity of the BD measurement method can approach the direct without surpassing it, because the BD time series is still expected to carry bunching noise of the same amplitude, as discussed in the previous paragraph. The situation is essentially the same for partially incoherent light, which we now turn to.

2.2. Partially incoherent light

If the light is partially incoherent, as is the case of the experiment we performed, then by the derivation shown in the Appendix (which contains the proof of all key formulae in this subsection) the ratios of (1) and (2) would become (ignoring the shot noise contribution

which is negligible because the beam has high occupation number)

$$\frac{\mathrm{cov}(S_k, S_l)}{\langle S_k\rangle^2} = \nu^2 e^{-t_{kl}^2/\tau^2}, \tag{10}$$

and

$$\frac{\mathrm{cov}(D_k^2, D_l^2)}{\langle D_k^2\rangle^2} = \nu^2 e^{-t_{kl}^2/\tau^2} + 2(1+\nu^2)\delta_{kl} \tag{11}$$

respectively, where $\nu \leq 1$ is the relative amplitude of incoherent fluctuations defined as

$$\nu = \frac{\sqrt{\mathrm{var}\langle S_j\rangle}}{\langle S_j\rangle}. \tag{12}$$

As will soon be discussed, the light we employed for our tests have $\nu < 1$ and $\nu^2 \ll 1$. Thus the covariance of the direct and BD time series S_k and D_k^2 should, by (10) and (11), respectively be a Gaussian of width τ and height ν^2, and the same Gaussian with a narrow central spike of of height $2(1+\nu^2)$ and spanning the width of one interval T.

The corresponding variances (4) and (5) are still evaluated by the same procedure as there (see Appendix), but now assume the (more general) expressions

$$\frac{\mathrm{var}\langle S_j\rangle}{\langle S_j\rangle^2} = \nu^2 \tag{13}$$

and this is the radiometer equation (direct detection sensitivity) of partially incoherent light, and

$$\frac{\mathrm{var}\langle D_j^2\rangle}{\langle D_j^2\rangle^2} = 2 + 3\nu^2; \tag{14}$$

while the long term variances now lead to the following form for their ensuing noise-to-signal ratios:

$$\frac{\mathrm{var}(\overline{S_\mathcal{T}})}{\langle \hat{S}_j\rangle^2} \approx \frac{\nu^2\sqrt{\pi}\tau}{\mathcal{T}} = \frac{\nu^2\sqrt{\pi}\tau}{NT}, \tag{15}$$

and

$$\frac{\mathrm{var}(\overline{D_\mathcal{T}^2})}{\langle \hat{D}_k^2\rangle^2} = \frac{\nu^2\sqrt{\pi}\tau}{NT} + \frac{2(1+\nu^2)}{N}. \tag{16}$$

Beware when $\nu^2 \ll 1$ *but* $N \gg 1$ is not too large, the $2(1+\nu^2)/N$ term of (16) that depicts the BD shot noise variance exceeds the bunching noise variance of the preceding term, despite the inequality $T \ll \tau$ which *always* applies to our sampling strategy. For *very* large N, the sensitivity of the BD method is governed by the first term on the right side of (16), as the last two terms become sub-dominant. Since the first term originated from the Gaussian autocorrelation of the BD time series, *viz.* the $\nu^2 e^{-t_{kl}^2/\tau^2}$ term of (11), this indicates the BD

signal is just as much contaminated by bunching noise as the direct (as (10) also has this term). Observe that when $\nu^2 \ll 1$, if N is not sufficiently large the $2(1+\nu^2)/N$ term of (16), depicting the BD shot noise variance, can exceed the BD bunching noise variance of the first term; this feature does not apply to fully incoherent light, where $\nu = 1$ and (7) reduces to (16). Ultimately it is the inability of the BD technique to remove or reduce the bunching noise in the original incident beam, that prevents one from employing this method to surpass the sensitivity limit of the radiometer equation.

In the case of partially incoherent light, as we shall see shortly, the bunching noise in both time series remain equal to each other in amplitude, while the shot noise exceeds the bunching noise in the BD time series even though it remains subdominant in the direct series.

3. The experiment

In the previous section we presented the status of recent quantum optics calculations as an extension of earlier semi-classical treatment of n-point correlation functions in which the amplitudes are classical c-numbers (*e.g.* Wang et al (1989)), and summarized their specific predictions of flux measurement sensitivity comparison between two methods. Despite the theoretical consensus among the 3 most recent papers on the subject: Zmuidzinas (2015); Lieu & Kibble (2015); Nair & Tsang (2015), there has not been any deliberate experimental verification of their predictions.

Previous experiments have, however, used similar experimental setups to characterize states of light. For example, the standard setup used for measuring the shot noise level in homodyne detection (in which the vacuum is chosen as the signal field and is mixed with a bright coherent state, known as the local oscillator) is identical to balanced detection of a coherent state. Homodyne detection has been used for many years to perform optical tomography Lvovsky & Babichev (2002); Smithey et al (1993) and has even been used previously to measure the photon-bunching characteristics of a given field Grosse et al (2007). Furthermore, a similar scheme has been used previously to produce random numbers through the measurement of vacuum fluctuations Shen et al (2010). In this experiment, the Fourier spectrum of the subtracted intensity was seen to have an autocorrelation function comprising a narrow central spike above a zero background, as one would expect from a coherent local oscillator. In contrast to these experiments, the method presented here involved the mixing between a thermal state of light with the vacuum field entering the empty port of the beamsplitter. Furthermore, the detection schemes vary significantly in the various experiments according the the information that one wishes to obtain.

In our experiment a direct comparison between the direct detection method and balanced detection for determining the flux of a given field is made. In order to provide a more meaningful comparison between the two methods, a stable reference field is also measured. Through comparison of the signals measured via balanced and direct detection with the measurements from the reference field, the performance of the two detection schemes is directly compared.

3.1. Basic setup and measurement strategy

An overview of the experimental layout is shown in Figure 2. The laser source is a low noise (RIO Grande) laser. An initial tap-off of a few percent from this field provided the *reference detection*. Any changes in average field power can be detected from this tap-off. Also note that the changes measured here will be proportional to any average field changes in the following detection schemes.

After this inital tap-off the field passes through a rotating glass disc and a pinhole. This setup is used to produce pseudo-thermal light following the method of Martienssen & Spiller (1964), with a photon bunching bandwidth of approximately 0.2 MHz. Note that the use of pseudo-thermal light is necessitated by the limitations of the experimental setup, as it is necessary to find a condition where the power in the field is high enough that the shot noise component is measurable, but also where the thermal noise component is not so large that it cannot be subtracted in the frequency band of interest. The effect of the plate on the time and frequency domains is shown in Figures 3 and 4 respectively. The state of light so produced has a relative amplitude of incoherent fluctuations

$$\nu \approx 0.15 \tag{17}$$

where ν was defined in (12). The properties of the pseudo-thermal light are chosen such that the limited subtraction of the balanced detector is sufficient to remove all of the classical noise in the frequency band of interest whilst ensuring that the average power through the pinhole is large enough such that the balanced detector can measure the shot noise level above the noise floor of the detector.

After the light is thermalised, another beamsplitter takes a tap-off of the pseudo-thermal light. This light is directed to a single detector where a *direct detection* is made. The light passing through the beamsplitter simultaneously undergoes a *balanced detection*. The balanced detector is used to subtract the classical (or photon bunching) noise and allow shot noise level measurements. A direct current subtraction method is used to maximise the subtraction afforded by the balanced detector Stefszky et al (2012). The output of the

balanced detector then undergoes high-pass filtering (at 1 MHz) in order to remove residual low-frequency noise sources, such as beam jitter Stefszky et al (2012). This setup allows us to make simulataneous comparisons between the average power in the (nearly) coherent reference field and the direct and balanced detection schemes.

The goal of the experiment is to track power changes of an incident laser field using both direct and balanced detection schemes simultaneously as illustrated in Figure 2. We are interested in the average flux of the field, rather than the fluctuations caused by the thermal nature of the light, and to this end the power exiting the laser is varied via control of the laser amplifier gain. In this way, the average power of the laser is halved from some initial value in 6 steps. The detected reference field provides an accurate measure of this change in power, as shown in Figure 5. At each of the six power levels 40,000 data points are recorded, resulting in a total of 240,000 data points. This entire measurement of 240,000 points is repeated at least two more times. For the analysis all of this data is concatenated (See Figure 5). This entire measurement procedure is completed with three different sampling intervals (of 0.167, 0.1 and 0.025 μs), such that the maximum frequency of the Fourier transforms of these frequencies are 3, 5 and 20 MHz respectively.

3.2. Photodetectors

All detectors used in the setup consist of a Hamamatsu G12180-003 (or two in the case of the BD) photodiode followed by a transimpedance gain stage and an output gain stage, both utilising AD829 opamps with a 15V supply. The output voltage of all devices is kept below **10V** to stay within the linear range of the opamp. All optical powers are also kept below the 6mW linear range limit of the photodiodes. The reference field detector has a 20k opamp gain stage, resulting in a bandwidth of around 6MHz and the maximum incident light power is approximately 200μW, while the direct detector has a 2k gain stage, giving a bandwidth of around 10 MHz, with a maximum incident power of 2mW (note that the power is varied in the measurements). The direct and reference detection are limited by the oscilloscope noise (which is approximately 3 orders below the signal level) as the dark noise levels of these detectors is below the electronic noise of the oscilloscope. The BD detector has two photodiodes in a current subtraction scheme (described in Stefszky et al (2012)) followed by a 20k transimpedance stage and a 1.2 MHz high pass filter before the output gain stage to remove residual noise at low frequencies. This scheme provides very high subtraction of up to 60 dB and a bandwidth of 6MHz, but does not allow for measurements of the photocurrents from the individual photodiodes.

All measurements are taken simultaneously using the same oscilloscope and the appro-

priate internal low pass filter is implemented to limit aliasing for all measurements. The measurements from both BD and DD detection schemes are compared to the reference detector in order to judge their performance. In this way it is possible to remove absolute errors that would otherwise be introduced, due to the fact that we need only measure the relative changes in flux. It is then of paramount importance that this detector is reliably operating in the linear regime, as all other measurements are referenced to the performance of this detector. As stated previously, to ensure that this is the case, no more than approximately 200μW is incident on the detector, and the output voltage under operation is limited to 10V. This ensures that both the photodiode and opamps are well within their linear operating range of 6mW and ≈13V respectively. The measured linearity of this detector is illustrated in Figure 7. The linear fit to the data has a gradient of 4.7×10^{-2} V/μW with a standard error of 1.5×10^{-4} V/μW and a p-value of 1.8×10^{-26}. It is evident that the detector is in the linear regime below around 300 μW of input power.

The slew rate requirements of the detectors are strictest on the DD scheme because the measured voltages are highest and the signal is strongly oscillating. In order to ensure that this detector was not slew rate limited it is simulated using TINA-TI SPICE. These results show that the expected slew rate SR of the DD detector is approximately 1V/70ns. From this value the standard slew rate definition can be used to determine the maximum amplitude V_{pk} of a sinusoid with frequency of $f = 20$MHz that can be reliably measured, which is found to be $SR/(2\pi f) \approx 115$mV. This is approximately one order of magnitude higher than the voltage changes seen in the detector on these timescales (50 ns).

Finally, the use of three detection schemes with varying gains, incident optical powers and designs, provides additional confidence in the performance of the detectors. Owing to the very different operational conditions of the three systems, measurements in which the results from two or more detectors coincide virtually guarantees that these detectors are operating in the nonlinear regime. This is because it is virtually impossible for two very different nonlinear systems to track one another over a wide range of inputs.

4. Bunching noise from shot noise measurement

We now show in Figure 6 the BD and direct time series when the data is binned to bin sizes of $N = 800$ in order to smooth out the variance of the variance of the measured shot noise, *i.e.* to suppress the effect of $2(1 + \nu^2)/N \approx 2/N$ term of (16) by letting N become large. In this way, each of the relatively high frequency fluctuations that were not part of the pedestal pattern of the laser light, Figure 5a, is due *solely* to photon bunching noise (note that there is essentially no shot noise in the direct time series because the incoherent light has

very high occupation number). It is then obvious that that the bunching noise as revealed by the direct and BD methods correlate very well, practically there is one-to-one correspondence between every peak and trough of fluctuation. It can also be seen, surprisingly, that the BD method seems to involve less bunching fluctuations. In fact, a least square test revealed that Figure 6b has a smaller χ^2 difference from Figure 5a than Figure 6a by ≈ 25 %. This difference could be for the reasons outlined in section 3.2, where it was demonstrated that nonlinearity in the direct detection process is a possible cause we have not succeeded in ruling out, even though the effect is unlikely to be large enough to account for the observed anomaly.

5. Correlation analysis

Next, we evaluate the covariance function of the time series, which in the case of direct detection is closely related to the bunching noise autocorrelation function often referred to as $g^{(2)}$. At each of the four sampling frequencies, the time series of the laser reference, direct, and BD measurements (the first two are shown in Figure 5 for the 3 MHz case) are simultaneously compared in this test.

According to the theoretical prediction, the covariance to mean-squared ratios of the direct and BD signals are, for stationary light, given by (10) and (11). And since $\nu^2 \ll 1$ by (17), this ratio for the square BD time series (*i.e.* the decontaminated measurement of D_j^2) should, by (11), have (a) a sharp central spike of magnitude ≈ 2, dropping rapidly to assume (b) the Gaussian function of the classical bunching noise in the direct current autocorrelation. We emphasize that we actually never measured a clean Gaussian in either the covariance function of the direct or squared BD time series, but a central broad peak and a long tail because of the existence of long range correlations in the bunching noise of the partially incoherent light we used (thus τ is really the minimum coherence scale among multiple ones). In fact, such correlations prevent the noise-to-signal ratio from assuming the simple $\propto \tau/(NT)$ form of the radiometer equation in (15) for large exposure times $NT \gg \tau$, because the presence of bunching noise components with timescales $> \tau$ modify the asymptotic form of radiation.

Next, all bunching noise components are expected to affect the BD time series in the same way as the direct, and so the first term on the right side of (16) should still be modified in the same way as the last term of (15). Any deviation of the BD noise-to-signal ratio from the direct ratio would imply a possible enhancement or suppression of bunching noise in the BD process, since the $2(1+\nu^2)/N$ term in (16) is negligible in the limit of large N.

Lastly, although the light signal we used is explicitly time varying, *viz.* it is periodic (having the pedestal time series of Figure 5 due to varying the laser output power), this non-stationarity occurs only on very long timescales and does not distort the small lag features of the covariance function on short timescales; rather, it only further extends the (already long) tail of the covariance function beyond that of the classical bunching noise of stationary light.

Turning to the graphs of Figure 8, it should be stated upfront that the sharp central spike referred to as (a) in the previous paragraph was *always* detected with the correct height in the squared BD time series (*viz.* the filtered measurement of D_j^2), and because this shot noise effect is insignificant when many samples are averaged, we will not show the spike. Instead, by avoiding the central two bins of the covariance data, we could reveal much more clearly what really matters, which is the effect listed as item (b) in the previous paragraph, *viz.* the shorter but much broader peak of the classical bunching noise. In this respect we shall find (below) that apart from the ignored small lags, the covariance to mean-squared ratio of the BD signal lies beneath the direct, but the difference becomes marginalized as one moves to lower sampling frequencies. Higher sampling frequency data seem to exhibit a greater difference between the direct and BD results (in terms of the latter involving a smaller bunching noise amplitude).

In Figure 8 we show the behavior in two such frequencies, 3 and 20 MHz, where the covariance to mean-squared ratio of the direct, BD squared, and source (laser) reference fluxes are all seen. Note the manner in which the residual BD shot noise spill-over at small lags quickly gives way to the bunching noise correlation (which is absent in the coherent laser signal, the long covariance tail there is entirely due to the periodic variation of the intrinsic laser power – the pedestal of Figure 5 – recalling that even 30,000 samples covers only 3/4 of a single laser power 'step' within which the laser intensity is held constant).

For the direct and BD detected incoherent light of the other two traces, however, this correlation power is smaller in the case of the BD than the direct. In fact, the covariance tail of the BD merges with the intrinsic effect of the reference signal's variation ahead of the direct. These effects, related to the reduced bunching noise in the BD time series mentioned in the end of the last section, become less marked as the sampling frequency increase to 5 MHz (which is still higher than the bunching noise frequency limit), *i.e.* overall we have good agreement between the two methods of detection, as expected by theory. Note also that the width of the bunching noise peak, *viz.* the tail after the initial drop, is less for the 20 MHz experiment than the 5 MHz, indicating that the bunching noise coherence length is

very crudely a constant [1] independent of the timing resolution of the data.

The performance of the direct and BD methods must further be compared in terms of the variance for a given sample size N, *i.e.* (15) and (16). This figure of merit is computed by bin-averaging the time series data, using a fixed N per bin $\mathcal{T}$. The results are shown in Figures 9 to 12, where we see that the BD method appears to do better by this metric. In section 3.2 we already discussed a possible reason for this, *viz.* the DD method suffers from nonlinearity problems. Even though the magnitude seems too small to account for the anomaly, we do not have any direct data to exclude it.

6. Discussion and conclusion

We carried out a detailed experimental investigation to compare the performance of direct versus BD measurement of the flux of incoherent light, with the latter inferring the flux from the shot noise variance of the light. Despite the potential problems of detector non-linearity (section 3.2), this is to the best of the authors' knowledge the first time that the bunching noise effect of high occupation number chaotic light via the shot noise of the field has successfully been measured, to the point of using it to infer the flux of the field. Furthermore, our data indicate that apart from the additional bunching noise component, the variance of the output of the BD deviates from the true (ensemble) flux only by virtue of the shot noise inherent to the BD subtraction.

The BD method was qualitatively found to involve the same level and pattern of bunching noise as the direct, in agreement with prior theoretical work Lieu & Kibble (2015); Nair & Tsang (2015); Zmuidzinas (2015). However, some BD measurements (20 MHz data) seemed to indicate a smaller noise amplitude in terms of photon bunching, whilst maintaining the noise pattern. This could be due to non-linearity in the DD process. As explained in section 3.2, even though simulations showed this should not be a problem, the conclusion was not quantitatively confirmed by measurements.

REFERENCES

Hanbury Brown, R., & Twiss, R.Q., 1957, Proc. Roy. Soc. A, 242, 300

[1] This is unlike the period of the reference signal variation, which is only constant in terms of the number of samples, *i.e.* 240,000 samples in six steps, after which the laser power is recycled to its original value in the next experiment.

Mandel, L., & Wolf, E., 1995, Optical coherence and quantum optics, Cambridge University Press.

Rice, F., 2016, Am. J. Phys., 84, 44

Lieu, R., and Kibble, T.W.B., 2015, Proc. of the 26th Symp. on Space Terahertz technology, paper W2-3 ((arXiv:1509.01868)

Martienssen, W. & Spiller, E., 1964, Coherence and fluctuations in light beams, Am. J. Phys., 32, 919

Nair, R., and Tsang, M., 2015, ApJ, 125, 6

Shen, Y., Tien, L., Zou, H., 2010, PRA, 81, 063814

Wang, L.J., Magill, B.E., & Mandel, L., 1989, J. Opt. Soc. Am., 6, 964

Zmuidzinas, J., 2015, Ap.J., 813, 17

Grosse, N.B., Symul, T., Stobinska, M., Ralph, T.C., Lam, P.K., 2007, PRL, 98, 153603

Stefszky, M.S., *et al*, 2012, CQG, 29, 145015.

Lvovsky, A. I., and Babichev, S. A., 2002, Phys. Rev. A, 66, 011801

Smithey, D. T., Beck, M., Raymer, M. G., and Faridani, A., 1993, Phys. Lett., 70, 1244

A. APPENDIX: Fluctuation of partially incoherent light

A.1. Directly detected signal

Here we derive the key formulae of section 2B (for the ones in section 2A, seeLieu & Kibble (2015)). The partially incoherent light may be modeled as a mixture of a coherent beam and chaotic beam. So long as we are dealing with a narrow bandwidth, it is more convenient to work with the Fourier transforms of the annihilation and creation operators,

$$\hat{a}(t) = \frac{1}{\sqrt{2\pi}} \int d\omega\, \hat{a}(\omega) e^{-i\omega t}; \hat{a}^\dagger(t) = \frac{1}{\sqrt{2\pi}} \int d\omega\, \hat{a}^\dagger(\omega) e^{i\omega t}. \tag{A1}$$

This preprint was prepared with the AAS LaTeX macros v5.2.

They satisfy the commutation relations

$$[\hat{a}(t), \hat{a}(t')] = \delta(t - t'). \tag{A2}$$

The intensity is $\omega_0 \hat{a}^\dagger(t)\hat{a}(t)$, but in the narrow-band case, it is simpler to remove the factor of ω_0, and talk instead about

$$\hat{J}(t) = \hat{a}^\dagger(t)\hat{a}(t), \tag{A3}$$

which represents the number of photons arriving per unit time. For the coherent state we assign the mean photon arrival rate (or expectation value of the same) as

$$\langle \hat{J}(t) \rangle_1 = (1 - \nu)\frac{n_0}{\tau}, \tag{A4}$$

and for the chaotic state

$$\langle \hat{J}(t) \rangle_2 == \nu\frac{n_0}{\tau}. \tag{A5}$$

The mean rate of the of the full beam,

$$\langle \hat{J}(t) \rangle = \langle \hat{J}(t) \rangle_1 + \langle \hat{J}(t) \rangle_2 = \frac{n_0}{\tau}, \tag{A6}$$

since intensity is additive.

Next, we evaluate the covariance of the intensity time series

$$\mathrm{cov}(J(t), J(t')) = \langle \hat{J}(t)\hat{J}(t') \rangle - \langle \hat{J} \rangle^2, \tag{A7}$$

where

$$\begin{aligned} \langle \hat{J}(t)\hat{J}(t') \rangle &= \langle \hat{a}^\dagger(t)\hat{a}(t)\hat{a}^\dagger(t')\hat{a}(t') \rangle \\ &= \langle \hat{a}^\dagger(t)\hat{a}(t') \rangle \delta(t - t') + \langle \hat{a}^\dagger(t)\hat{a}^\dagger(t')\hat{a}(t)\hat{a}(t') \rangle. \end{aligned} \tag{A8}$$

For the coherent state the expectation value of the two point function is

$$\langle \hat{J}(t)\hat{J}(t') \rangle_1 = (1 - \nu)\frac{n_0}{\tau}\delta(t - t') + (1 - \nu^2)\frac{n_0}{\tau}. \tag{A9}$$

Thus the covariance is

$$\mathrm{cov}(J(t), J(t'))_1 = (1 - \nu)\frac{n_0}{\tau}\delta(t - t') \tag{A10}$$

which clearly shows the coherent state has only shot noise and no bunching noise. Repeating the exercise to the chaotic state, assuming it is Gaussian thermal light the last term in (A8) is expressible as

$$\begin{aligned} \langle \hat{a}^\dagger(t)\hat{a}^\dagger(t')\hat{a}(t)\hat{a}(t') \rangle &= \langle \hat{a}^\dagger(t)\hat{a}(t) \rangle \langle \hat{a}^\dagger(t')\hat{a}^\dagger(t') \rangle \\ &\quad + \langle \hat{a}^\dagger(t)\hat{a}(t') \rangle \langle \hat{a}^\dagger(t')\hat{a}^\dagger(t) \rangle. \end{aligned} \tag{A11}$$

As a result

$$\mathrm{cov}(J(t), J(t'))_2 = \nu \frac{n_0}{\tau}\delta(t-t') + \nu^2 \frac{n_0^2}{\tau^2} e^{-(t-t')^2/\tau^2}. \tag{A12}$$

Since the two constituent beams 1 and 2 are uncorrelated, the covariance of the full beam is the just the sum of the two covariances, *viz.*

$$\mathrm{cov}(J(t), J(t')) = \frac{n_0}{\tau}\delta(t-t') + \nu^2 \frac{n_0^2}{\tau^2} e^{-(t-t')^2/\tau^2}. \tag{A13}$$

This is the derivation of the complete version of (10) in section 2B which includes the shot noise contribution, *viz.* the first term on the right side of (A13), as well as the bunching noise. By combining (A13) with (A7) and (A8), we arrive at

$$\langle \hat{a}^\dagger(t)\hat{a}^\dagger(t')\hat{a}(t)\hat{a}(t')\rangle = \frac{n_0^2}{\tau^2}(1+\nu^2 e^{-(t-t')^2/\tau^2}), \tag{A14}$$

an equation we shall find useful in due course.

If we define the average total flux over some time interval T as

$$\hat{J}_T(t) = \frac{1}{T}\int_{t-T}^{t} dt'\, \hat{J}(t'), \tag{A15}$$

then we find

$$\mathrm{var}(J_T(t)) = \frac{1}{\tau T}\left[\nu^2 n_0^2 F\left(\frac{T}{\tau}\right) + n_0\right], \tag{A16}$$

where

$$F\left(\frac{T}{\tau}\right) = \frac{\tau}{T}\int_{-T}^{T} dt\,(T-|t|)|f(t)|^2. \tag{A17}$$

Note that if $T \ll \tau$, the function $f(t)$ in the integrand will be reduced to $1/\tau^2$, so $F(T/\tau) \approx T/\tau$. The relative uncertainty in the measurement of J_T is given by

$$\frac{\mathrm{var}(J_T(t))}{\langle \hat{J}_T(t)\rangle^2} = \frac{\tau}{T}\left[\nu^2 F\left(\frac{T}{\tau}\right) + \frac{1}{n_0}\right], \tag{A18}$$

or

$$\frac{\mathrm{var}(J_T(t))}{\langle \hat{J}_T(t)\rangle^2} \approx \nu^2 + \frac{\tau}{n_0 T}, \quad \text{for} \quad T \ll \tau \tag{A19}$$

which agrees with (13) if we ignore the shot noise contribution of the last term. On the other hand, if we measure for a much longer time $\mathcal{T} = NT$, we must replace T in (A15) by $\mathcal{T}$ and use the limiting value of $F(x)$ for $x \gg 1$, *viz* $\sqrt{\pi}$. Then we have, dropping the shot noise term,

$$\frac{\mathrm{var}(J_\mathcal{T}(t))}{\langle \hat{J}_\mathcal{T}(t)\rangle^2} \approx \sqrt{\pi}\frac{\nu^2\tau}{\mathcal{T}} = \sqrt{\pi}\frac{\nu^2\tau}{NT}, \quad \text{for} \quad \mathcal{T} \gg \tau. \tag{A20}$$

and this is the derivation of (15).

A.2. Difference signal for split beam

In a 50:50 beam splitter, it is useful to consider a second input beam, which is in fact in its vacuum state. Let us represent the annihilation and creation operators of that second input by $\hat{b}(t), \hat{b}^\dagger(t)$. Then for the two output beams we have annihilation operators

$$\hat{c} = \frac{1}{\sqrt{2}}(\hat{a} + i\hat{b}), \qquad \hat{d} = \frac{1}{\sqrt{2}}(\hat{a} - i\hat{b}). \tag{A21}$$

Note that $\hat{c}$ and $\hat{d}$ each satisfy the commutation relations (A2), and also (A3) and (A6) with n_0 replaced by $n_0/2$ in the latter. Moreover, $\left[\hat{c}, \hat{d}^\dagger\right] = 0$.

One might perhaps wonder if using $\hat{b}(t)$ rather than $\hat{b}(\omega)$, with the replacement of factors of ω by ω_0, which is justified for the narrow-bandwidth case, might be inadmissible for the vacuum contribution. However, if one retains the factors of ω, they will be converted to time derivatives that will ultimately act on other factors that are limited by bandwidth, and the leading contributions will be given quite accurately by the replacement of ω by ω_0, so should not be a serious problem.

The quantity we are particularly interested in is the difference signal, the difference between the numbers of photons arriving in the two output channels. This is given by

$$\hat{D}(t) = \hat{c}^\dagger(t)\hat{c}(t) - \hat{d}^\dagger(t)\hat{d}(t). \tag{A22}$$

Substituting from (A21) we see that this quantity may be written as

$$\hat{D}(t) = i\hat{a}^\dagger(t)\hat{b}(t) - i\hat{b}^\dagger(t)\hat{a}(t). \tag{A23}$$

Obviously, its expectation value is zero:

$$\langle \hat{D}(t) \rangle = 0. \tag{A24}$$

The factorization between $\hat{a}$ and $\hat{b}$ operators makes this a very convenient form to use. For example, in computing the two-time function, we see that

$$\langle \hat{D}(t)\hat{D}(t') \rangle = \langle \hat{a}^\dagger(t)\hat{a}(t') \rangle \langle \hat{b}(t)\hat{b}^\dagger(t') \rangle + \langle \hat{a}(t)\hat{a}^\dagger(t') \rangle \langle \hat{b}^\dagger(t)\hat{b}(t') \rangle, \tag{A25}$$

and because the b input is in its vacuum state, the second term vanishes, while in the first, $\langle \hat{b}(t)\hat{b}^\dagger(t') \rangle = \delta(t - t')$. Thus we find

$$\mathrm{cov}(D(t), D(t')) = \langle \hat{D}(t)\hat{D}(t') \rangle = \frac{n_0}{\tau}\delta(t - t'). \tag{A26}$$

So the measurement of the variance of D provides a way of measuring n_0.

Of course, any measurement will take up a finite time interval. We suppose as before that the total available time $\mathcal{T}$ is divided up into N small segments of duration T, and define the average flux in the jth interval as

$$\hat{D}_j = \frac{1}{T}\int_{(j-1)T}^{jT} dt\, \hat{D}(t), \tag{A27}$$

where we assume $T \ll \tau$, so that

$$\mathrm{var}(D_j) = \frac{n_0}{T\tau}, \qquad \mathrm{cov}(D_j, D_k) = 0,\ (j \neq k). \tag{A28}$$

Now to estimate the accuracy of the measurement we can make, we need to compute the expectation value $\langle \hat{D}_j^2 \hat{D}_k^2 \rangle$. However, for use later we consider the more general case

$$\begin{aligned}\langle \hat{D}_j \hat{D}_k \hat{D}_l \hat{D}_m \rangle &= \frac{1}{T^4}\int_{(j-1)T}^{jT} dt_1 \int_{(k-1)T}^{kT} dt_2 \\ &\quad \int_{(l-1)T}^{lT} dt_3 \int_{(m-1)T}^{mT} dt_4 \langle \hat{D}(t_1)\hat{D}(t_2)\hat{D}(t_3)\hat{D}(t_4)\rangle. \end{aligned}\tag{A29}$$

When we substitute from (A23), each term in the expectation value can be written as a product of an expectation value of $\hat{a}$ and $\hat{a}^\dagger$ operators, and one of $\hat{b}$ and $\hat{b}^\dagger$ operators. Moreover, the latter vanish if they have a $\hat{b}$ on the right or a $\hat{b}^\dagger$ on the left, and there must be equal numbers of each of the two terms in (A23) containing $\hat{b}$ and $\hat{b}^\dagger$ operators. So there are just two terms remaining:

$$\begin{aligned}&\langle \hat{D}(t_1)\hat{D}(t_2)\hat{D}(t_3)\hat{D}(t_4)\rangle \\ =\ &\langle \hat{a}^\dagger(t_1)\hat{a}^\dagger(t_2)\hat{a}(t_3)\hat{a}(t_4)\rangle \times \langle \hat{b}(t_1)\hat{b}(t_2)\hat{b}^\dagger(t_3)\hat{b}^\dagger(t_4)\rangle \\ &+\langle \hat{a}^\dagger(t_1)\hat{a}(t_2)\hat{a}^\dagger(t_3)\hat{a}(t_4)\rangle \times \langle \hat{b}(t_1)\hat{b}^\dagger(t_2)\hat{b}(t_3)\hat{b}^\dagger(t_4)\rangle. \end{aligned}\tag{A30}$$

With the abbreviation $t_{jk} = t_j - t_k$, we see that

$$\langle \hat{b}(t_1)\hat{b}(t_2)\hat{b}^\dagger(t_3)\hat{b}^\dagger(t_4)\rangle = \delta(t_{13})\delta(t_{24}) + \delta(t_{14})\delta(t_{23}), \tag{A31}$$

while

$$\langle \hat{b}(t_1)\hat{b}^\dagger(t_2)\hat{b}(t_3)\hat{b}^\dagger(t_4)\rangle = \delta(t_{12})\delta(t_{34}), \tag{A32}$$

so clearly the result will only be nonzero when the indices (j,k,l,m) are equal in pairs.

Enlisting the last two equations and (A14), we see the first term on the right side of (A30) is

$$\begin{aligned}&\hat{a}^\dagger(t_1)\hat{a}^\dagger(t_2)\hat{a}(t_3)\hat{a}(t_4)\rangle\langle \hat{b}(t_1)\hat{b}(t_2)\hat{b}^\dagger(t_3)\hat{b}^\dagger(t_4)\rangle \\ =\ &\delta(t_{13})\delta(t_{24})\langle \hat{a}^\dagger(t_1)\hat{a}^\dagger(t_2)\hat{a}(t_1)\hat{a}(t_2)\rangle + \\ &\quad \delta(t_{14})\delta(t_{23})\langle \hat{a}^\dagger(t_1)\hat{a}^\dagger(t_2)\hat{a}(t_2)\hat{a}(t_1)\rangle \\ =\ &\frac{n_0^2}{\tau^2}(1+\nu^2 e^{-t_{12}^2/\tau^2})[\delta(t_{13})\delta(t_{24}) + \delta(t_{14})\delta(t_{23})]; \end{aligned}\tag{A33}$$

and the second term is

$$\begin{aligned}
& \langle \hat{a}^\dagger(t_1)\hat{a}(t_2)\hat{a}^\dagger(t_3)\hat{a}(t_4)\rangle \langle \hat{b}(t_1)\hat{b}^\dagger(t_2)\hat{b}(t_3)\hat{b}^\dagger(t_4)\rangle \\
= \; & \langle \hat{a}^\dagger(t_1)\hat{a}^\dagger(t_3)\hat{a}(t_1)\hat{a}(t_3)\rangle \delta(t_{12})\delta(t_{34}) + \\
& \quad \langle \hat{a}^\dagger(t_2)\hat{a}(t_3)\rangle \delta(t_{12})\delta(t_{23})\delta(t_{34}) \\
= \; & \frac{n_0^2}{\tau^2}(1+\nu^2 e^{-t_{13}^2/\tau^2})\delta(t_{12})\delta(t_{34}) + \\
& \quad \frac{n_0}{\tau}\delta(t_{12})\delta(t_{23})\delta(t_{34}).
\end{aligned} \tag{A34}$$

Note the symmetry of this expression under permutations of $\{1,2,3,4\}$, which results from the fact that the different $\hat{D}_j$ operators commute with each other.

Substituting (A33) and (A34) into (A30), and integrating over short time intervals, $T \ll \tau$ as in (A29), we find (bearing in mind the symmetry under the aforementioned permutations),

$$\begin{aligned}
& \langle \hat{D}_j \hat{D}_k \hat{D}_l \hat{D}_m \rangle \\
= \; & \delta_{jk}\delta_{lm}\frac{n_0^2}{T^2\tau^2}(1+\nu^2 e^{-t_{jl}^2/\tau^2}) + \delta_{jl}\delta_{km}\frac{n_0^2}{T^2\tau^2}(1+\nu^2 e^{-t_{jk}^2/\tau^2}) + \\
& \delta_{jm}\delta_{kl}\frac{n_0^2}{T^2\tau^2}(1+\nu^2 e^{-t_{jk}^2/\tau^2}) + \delta_{jk}\delta_{kl}\delta_{lm}\frac{n_0}{T^3\tau},
\end{aligned} \tag{A35}$$

where $t_{jk} = (j-k)T$.

To obtain the covariance of D_j^2 and D_l^2, we set $k = j$ and $m = l$, and remove the first of the seven terms in (A35), since the term is canceled by the product of expectation values. This yields

$$\mathrm{cov}(D_j^2, D_l^2) = \frac{n_0^2}{T^2\tau^2}\nu^2 e^{-t_{jl}^2/\tau^2} + \frac{n_0^2}{T^2\tau^2}2(1+\nu^2)\delta_{jl} + \delta_{jl}\frac{n_0}{T^3\tau}. \tag{A36}$$

This is the derivation of the complete version of (11) that includes the shot noise in the original (unsplit) beam as the last term of (A36). The first term alone gives the covariance when $j \neq l$. For $j = l$ we find

$$\mathrm{var}(D_j^2) = (2+3\nu^2)\frac{n_0^2}{T^2\tau^2} + \frac{n_0}{T^3\tau}. \tag{A37}$$

Thus the fractional error is given by

$$\frac{\mathrm{var}(D_j^2)}{\langle \hat{D}_j^2 \rangle^2} = (2+3\nu^2) + \frac{\tau}{n_0 T}. \tag{A38}$$

This is the derivation of the full version of (14) that includes the shot noise variance $\tau/(n_0 T)$ in the original (unsplit) beam as well.

Of course, as before we can do better by observing for a longer time and computing the sample mean

$$\overline{D^2} = \frac{1}{N}\sum_{j=1}^{N} D_j^2. \tag{A39}$$

Clearly,

$$\mathrm{var}(\overline{D^2}) = \frac{1}{N^2}\sum_{j,l=1}^{N} \mathrm{cov}(D_j^2, D_l^2). \tag{A40}$$

When we substitute from (A36), in the first term, we can convert the sum over $j - l$ to a Gaussian integral:

$$\sum_j e^{-j^2T^2/\tau^2} \approx \frac{1}{T}\int dt\, e^{-t^2/\tau^2} = \frac{\sqrt{\pi}\tau}{T}. \tag{A41}$$

Thus we obtain

$$\frac{\mathrm{var}(\overline{D^2})}{\langle \hat{D}_j^2\rangle^2} = \frac{1}{N}\left[\frac{\nu^2\sqrt{\pi}\tau}{T} + 2(1+\nu^2) + \frac{\tau}{n_0 T}\right]. \tag{A42}$$

This is the derivation of the full version of (16) that includes the shot noise variance in the original (unsplit) beam as the last term.

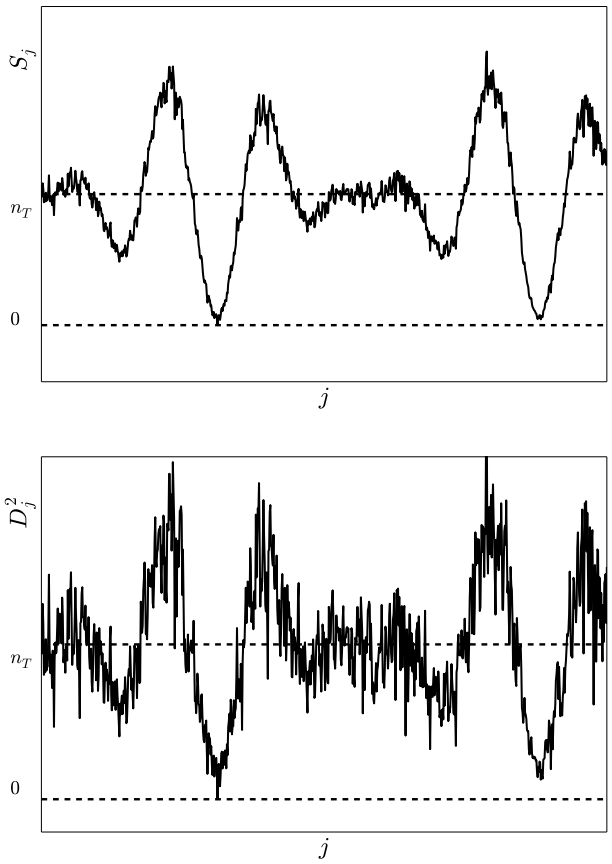


Fig. 1.— Theoretically expected noise characteristics of the intensity of stationary thermal radiation as measured directly, and via a balanced (*i.e.* 50:50) beam-splitter detection technique referred to as BD in the text. The x-axis gives the data sample index (hence time, assuming the data are sampled time contiguously and at equal intervals), and the y-axis the incident light intensity measured by the two methods: direct is the top graph and BD the bottom. Note the BD squared intensity difference D_j^2 between the two split beams, which equals (in terms of photons counts per bin) to the variance *and* also the ensemble average of the intensity S_j of the primary incident beam, still exhibits classical bunching noise that correlates with the direct intensity time series. Additionally the former is also expected to have more shot noise. This figure illustrates why D_j^2 is a measure of the primary incident flux as well as S_j. The BD method can theoretically be as sensitive as the direct, but cannot surpass it.

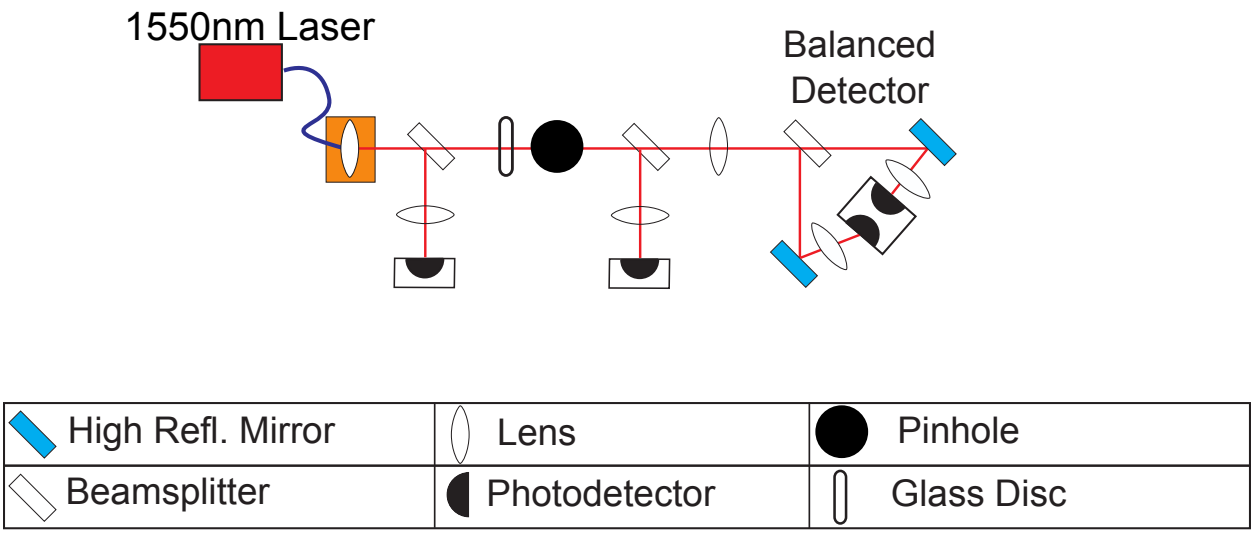


Fig. 2.— Experimental layout for the near simultaneous flux measurements of a beam of coherent light . The ground glass is rotated off (optical) axis to produce pseudo-thermal, or partially incoherent, light with classical bunching noise extending to $\sim 1-2$ MHz via scattering. The photodetectors are described in more detail in the text. In such a setup, the directly measured flux of the laser light serves as the reference flux; against which the flux of the same light after it loses coherence (as a result of passage through the ground glass), as measured by the direct and BD detection methods, are compared.

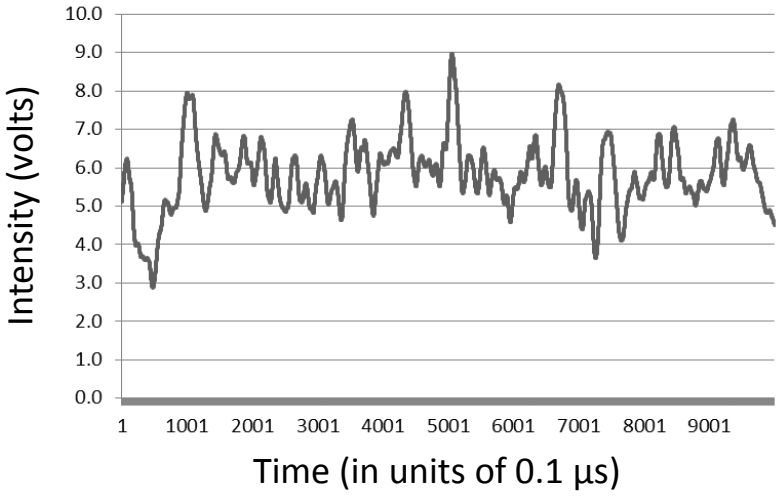


Fig. 3.— The time series of partially incoherent light as detected by the direct detection scheme, with the classical bunching noise generated by a rotating ground glass plate, see Figure 2. The light is partially incoherent because the ratio ν of the standard deviation to the mean intensity (see (12) and (17)) is less than unity. This type of light is used in our experimental tests of the sensitivity of direct versus BD flux measurement technique.

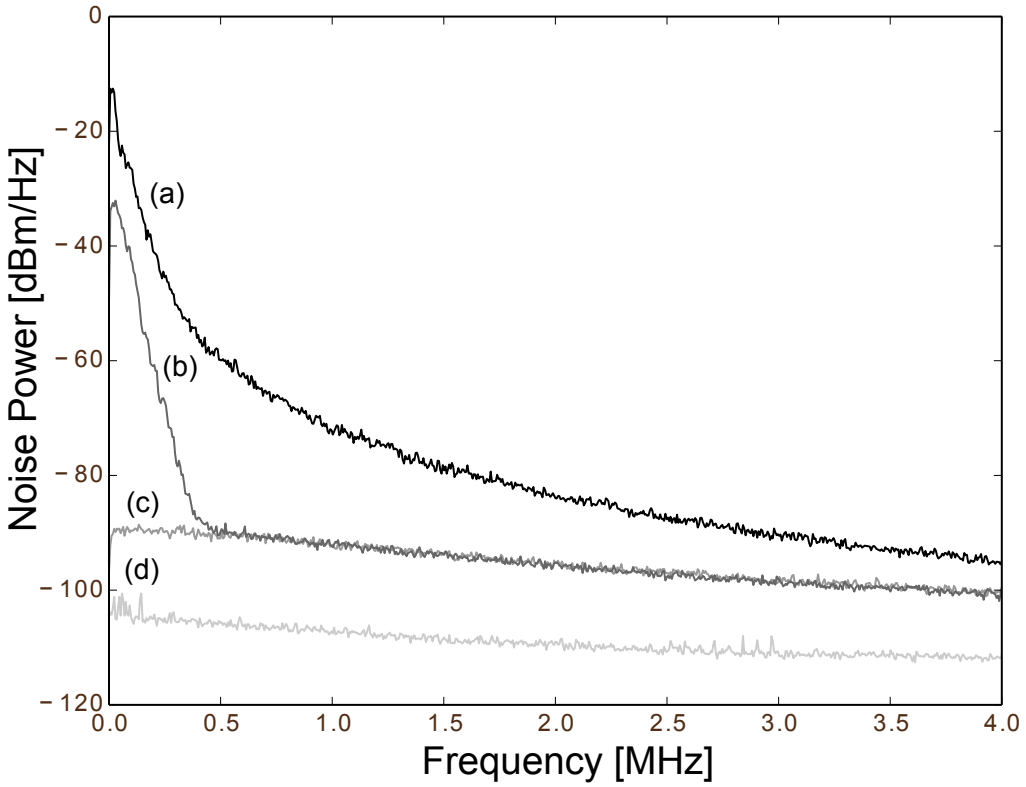


Fig. 4.— Spectra of the BD detector output voltage with different fields incident on the diodes showing typical characteristics of the fields. Trace (a) is the noise spectrum of the pseudo-thermal light (passing through the rotating plate), when all the incident power is on a single diode. Trace (b) is the pseudo-thermal light noise spectrum when the optical power is distributed equally between both diodes and BD subtraction is at a maximum. Trace (c) is when the rotating plate is removed and the power is equal on both diodes such that the shot noise of the coherent field is measured. Trace (d) is the dark noise of the detection system, whereby no light is incident on the detectors. The incident power for traces (a),(b), and (c) are equal. Note how both (b) and (c) merge at the shot noise level when frequencies are high. All traces were taken on a spectrum analyzer with an RBW of 3 kHz and VBW of 10 Hz. In order to show the dark noise clearance no gain correction was applied to the traces, which is why the shot noise asymptote is not flat. This figure shows how the shot noise level reached (at high frequencies) by the BD flux measurement method stands sufficiently above the dark noise (DN clearance is a minimum of 8dB at 20MHz)

.

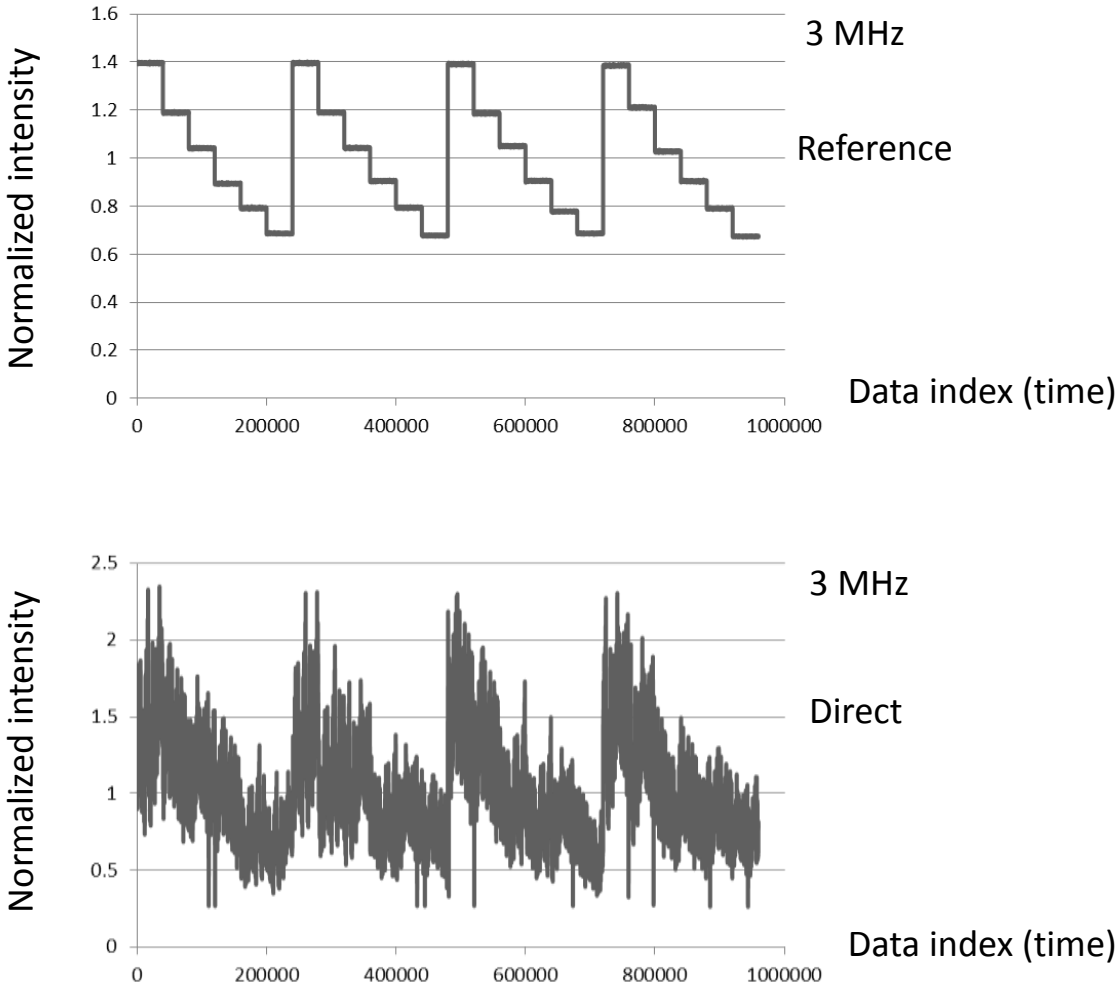


Fig. 5.— The entire (concatenated) data run with a sampling interval of 0.167 μs, as measured via the reference detector (top) and direct detector after passing through the rotating disc (bottom). The data from the reference detector shows how the laser power varies over time, and the data from the direct detector (bottom) shows the effect of photon-bunching contamination due to the rotating disc. All intensities shown are normalized to a mean of unity over the entire time series.

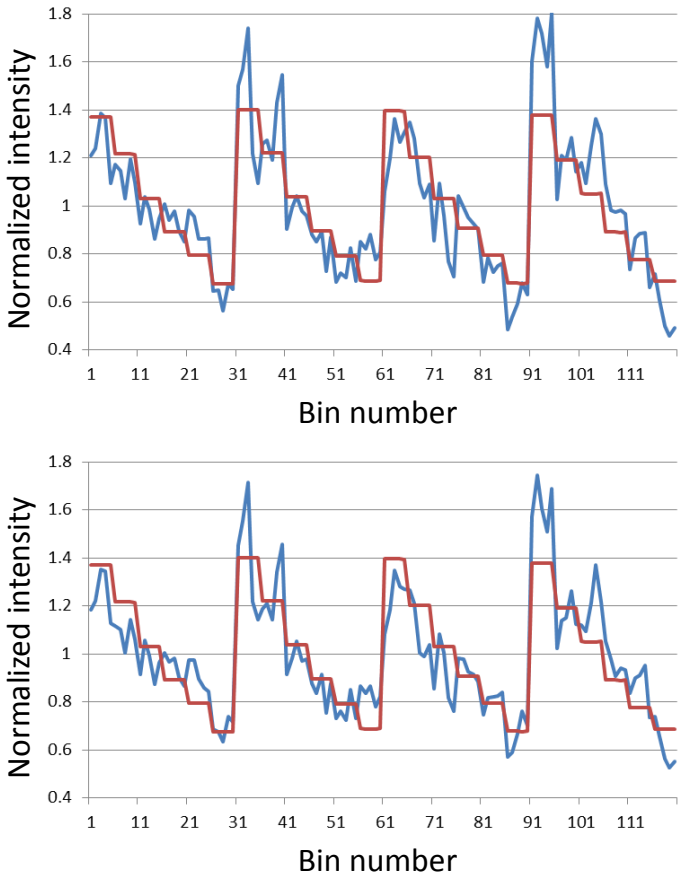


Fig. 6.— The direct (top blue) and BD (bottom blue) time series with sampling interval of 0.025 μs, and bin-averaged every 800 (*i.e.* $N = 800$) of the 960,000 samples. The BD time series is obtained after the Fourier transform, filtering and then inverse Fourier transform. The two series are to be compared to the underlying directly measured coherent reference signal (red). Note that each small wiggle superimposed upon the underlying pedestal is due to bunching noise, as the largeness of N ensured that the shot noise component in the BD is ironed out (this component is negligible in the direct series irrespective of the size of N). The r.m.s. percentage difference between the BD flux and reference flux is 1.57 % over the entire time series, while the same between direct and reference is > 50 % higher, *viz.* 2.37 %.

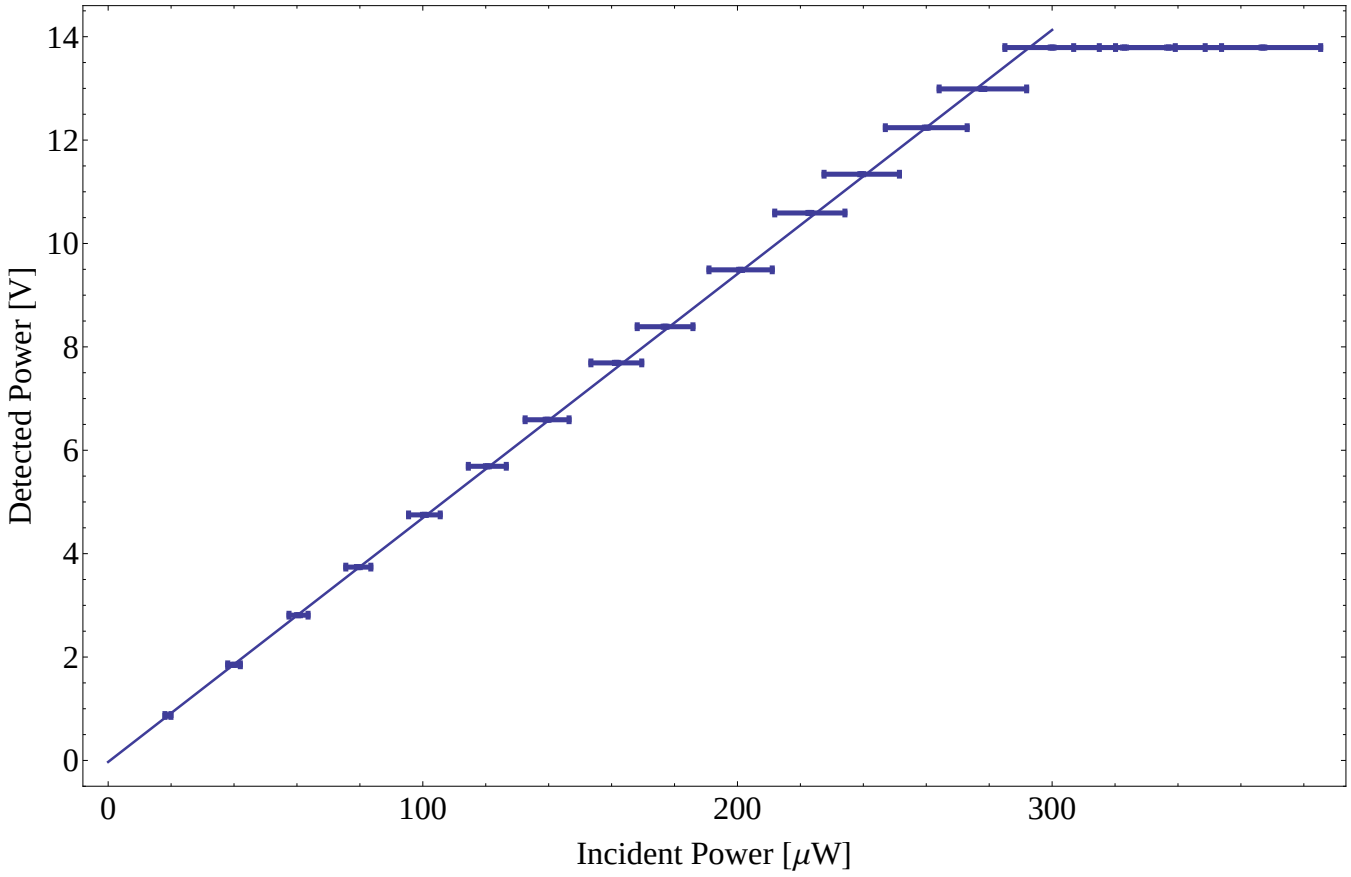


Fig. 7.— Measured linearity of the reference detector. The power before incidence (measured using a Thorlabs S132C detector with 5% uncertainty) is compared to the power measured converting the photodetector voltage.

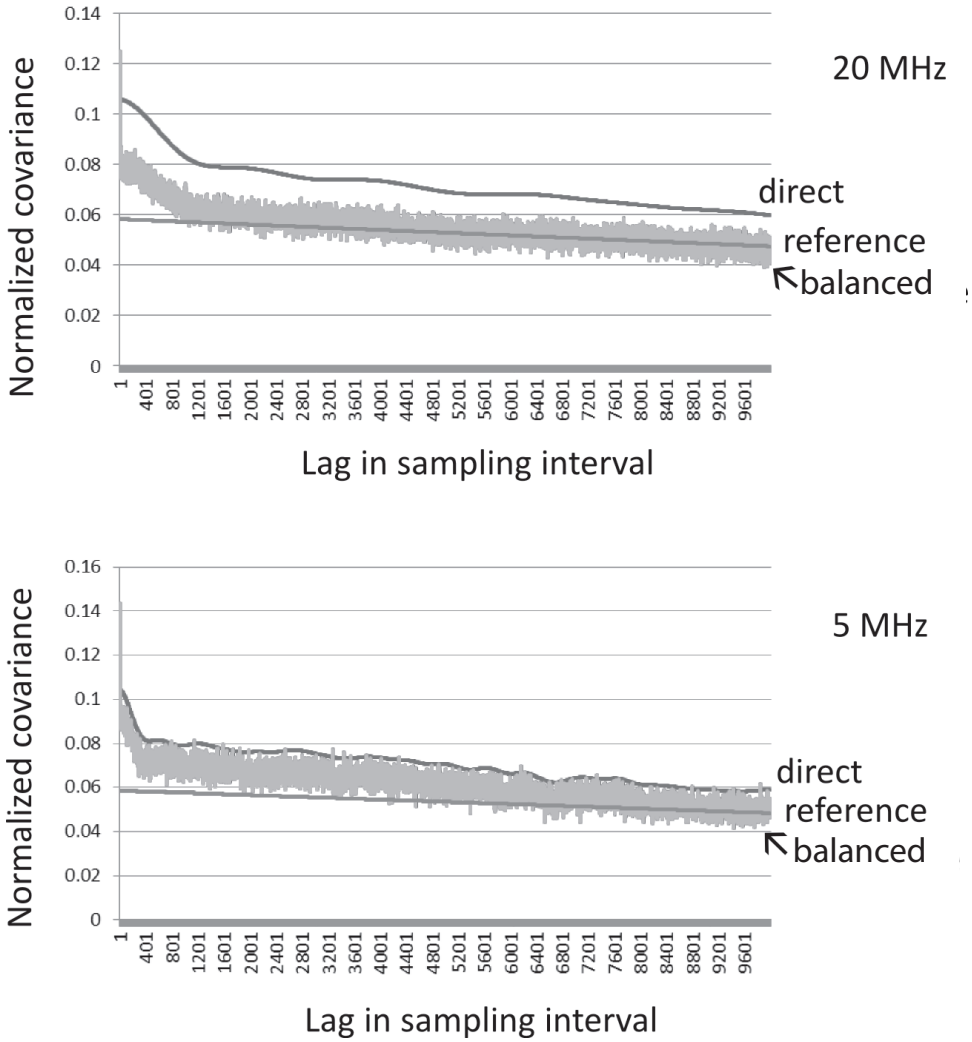


Fig. 8.— The correlation measurements of the direct, BD squared (lightest color), and reference signals for two sampling frequencies. The normalized covariance is defined as the covariance divided by the product of the means, *i.e.* $\mathrm{cov}(A,B)/\langle A\rangle\langle B\rangle$ where $\mathrm{cov}(A,B) = \langle AB\rangle - \langle A\rangle\langle B\rangle$ and the ensemble mean $\langle\cdots\rangle$ is estimated by the sample mean. The central two lag intervals are omitted from all data to avoid the very tall shot noise peak in the BD squared signal, *viz.* the $2\delta_{kl}$ term of (11) (there is some spill-over into the next several bins, resulting in the much shorter spike on the extreme left). Both the direct and BD correlation functions have a long tail above the reference level, indicating that the width τ of the central Gaussian-like peak is actually the minimum coherence time, *i.e.* there are other (larger) coherence scales present in the bunching noise. The suppression of the correlation power of the BD squared signal relative to the direct signal is evident. It indicates the BD process reduces bunching noise, more so at higher sampling frequencies, contrary to theoretical predictions.

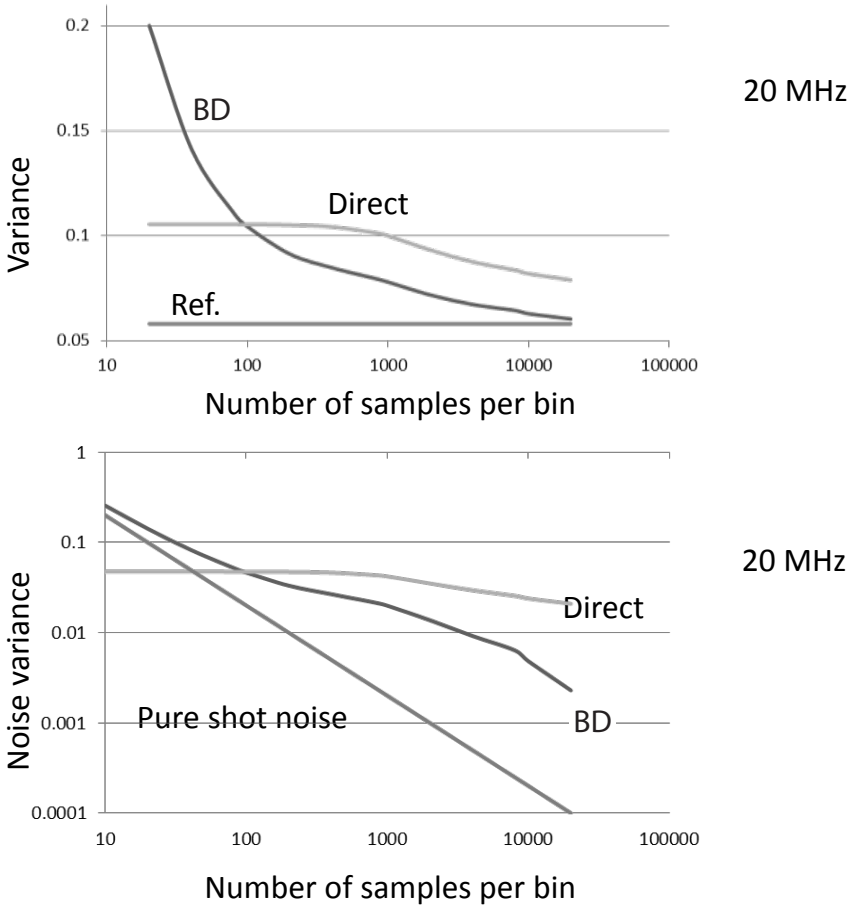


Fig. 9.— Variance in the direct time series of the coherent reference source and the direct and BD detected time series of the same after the light partially lost coherence (all variances are defined by the left side of (15) and (16)), each series is sampled at the interval of 0.025 μs (resulting in a maximum Fourier frequency of 20 MHz), and bin-averaged into various large time intervals given by the x-axis. Each variance is normalized to the mean-squared flux for meaningful comparison. Note that the excess variances above the laser reference value are due to bunching noise only in the direct, and shot noise and bunching noise in the BD (with latter assuming prominence only towards smaller number of samples per bin, N), signals. This excess noise variance is plotted in the lower graph.

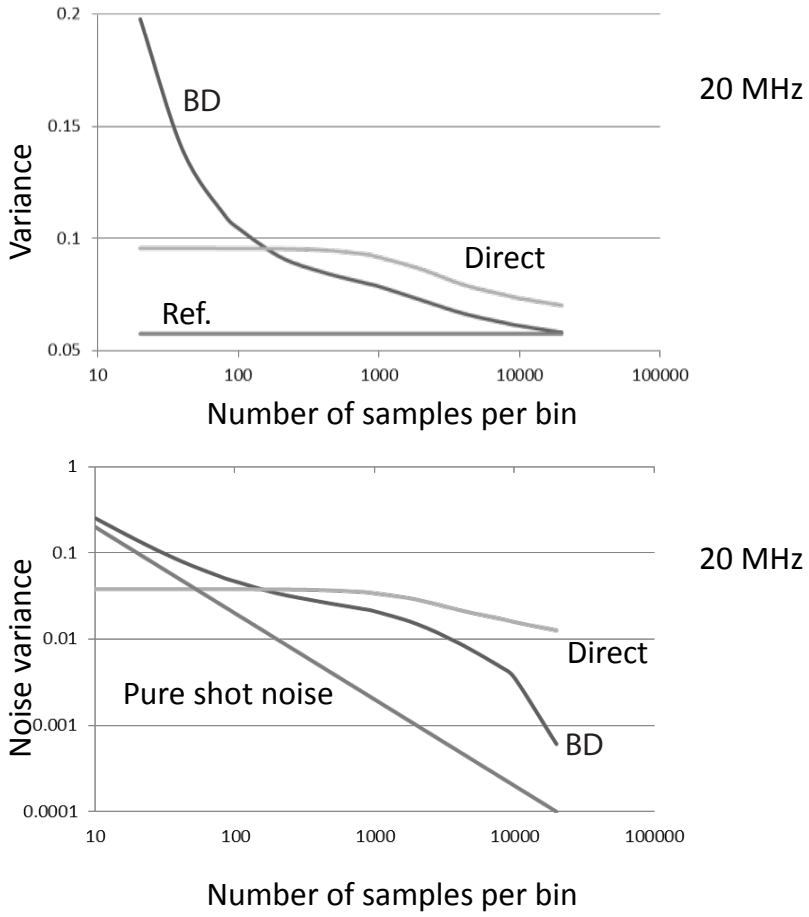


Fig. 10.— As in Figure 9, except for an independent data set of 720,000 samples, also acquired with a sampling interval of 0.025 μs.

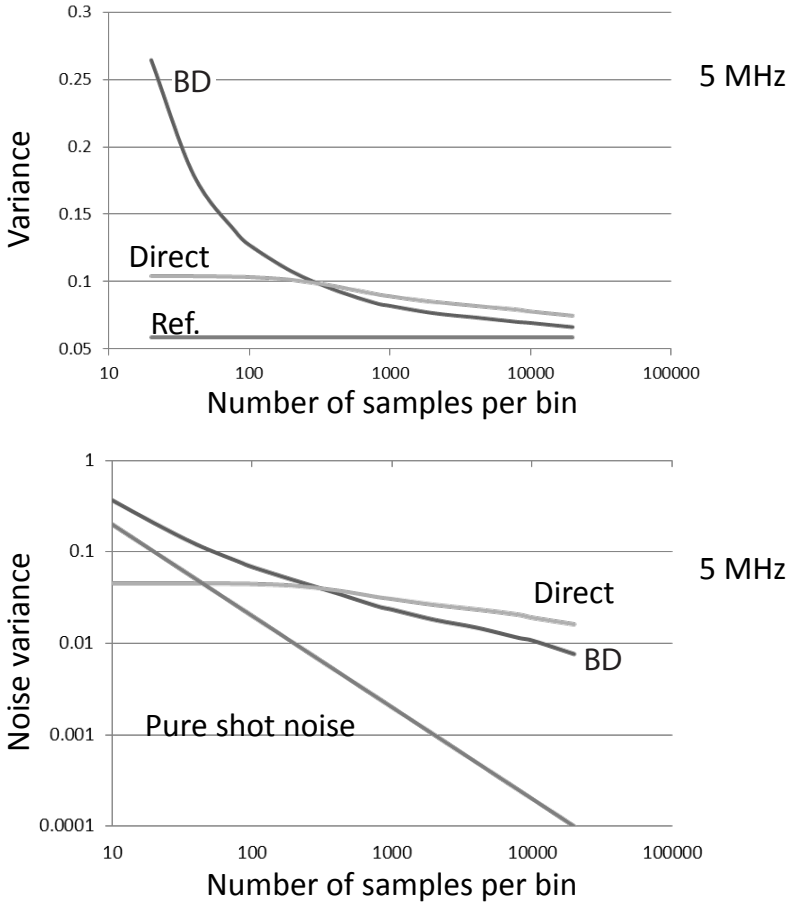


Fig. 11.— As in Figure 9, except for an independent data set of 720,000 samples acquired at the sampling interval of 0.1 μs (maximum Fourier frequency of 5 MHz). Note how the reduction in the BD variance w.r.t. the direct for large bin sizes is not as marked as in the 20 MHz sampling case of Figures 9 and 10.

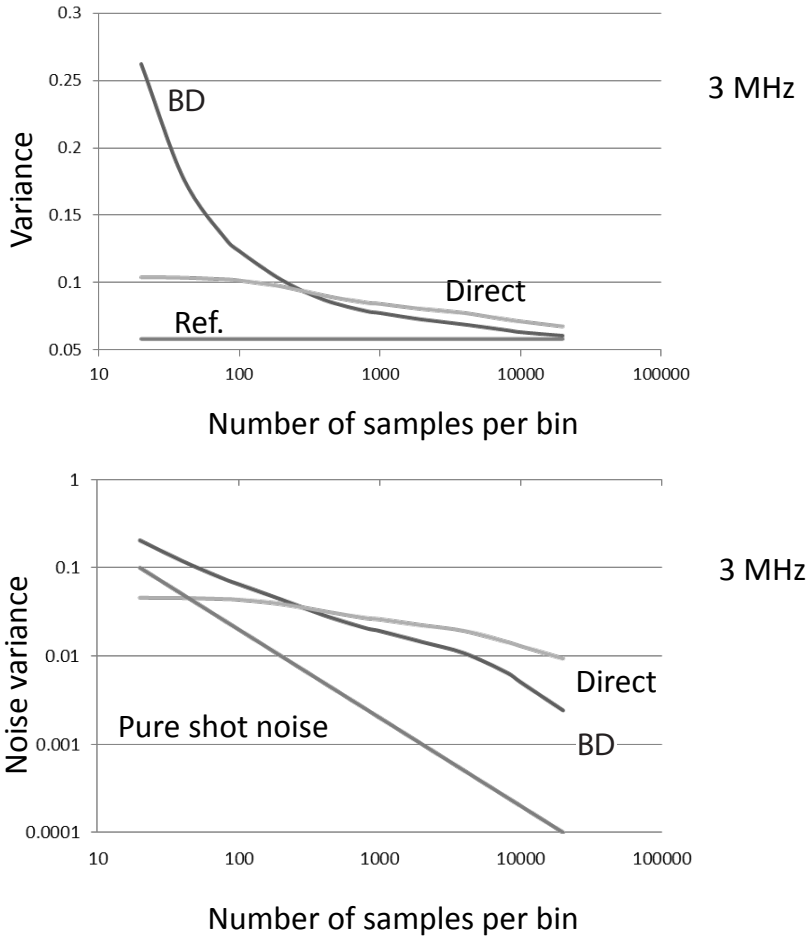


Fig. 12.— As in Figure 9, except for an independent data set of 960,000 samples acquired at the sampling interval of 0.167 μs (maximum Fourier frequency of 3 MHz). Note how the reduction in the BD variance w.r.t. the direct for large bin sizes is not as marked as in the 20 MHz sampling case of Figures 9 and 10. Thus there seems to be an advantage in sampling as much below the coherence time τ of the bunching noise as possible.

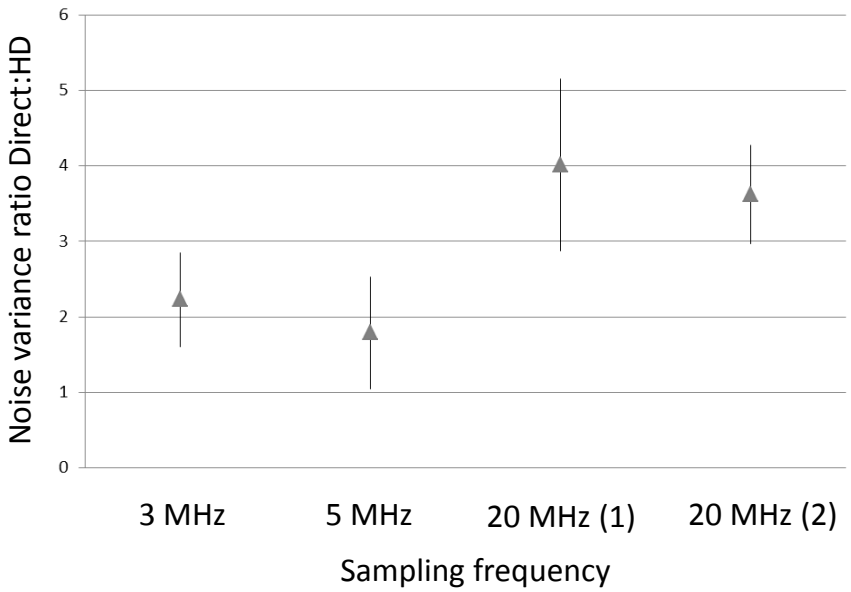


Fig. 13.— The ratio r of the bunching noise variance, direct to BD, in the case when the time series is bin-averaged every 800 (*i.e.* $N = 800$), as a function of sampling frequency. The error in the ratio is obtained by computing the variance in this ratio from the data. Quantum field theory Zmuidzinas (2015); Lieu & Kibble (2015); Nair & Tsang (2015) predicts $r = 1$ for large N (the values of N used in this graph satisfy the large N condition), *i.e.* there should be no difference in sensitivity between the two methods. The graph is consistent with the partial reduction of the bunching noise by the BD process first noted in Figure 8, but the effect is quite marginal (due to the large errors in r), especially towards lower sampling frequencies.